

DETERMINING TROPICAL CYCLONE CENTER LOCATION WITH CYGNSS WIND SPEED MEASUREMENTS

David Mayers¹, Chris Ruf²

- (1) Applied Physics Program, University of Michigan, Ann Arbor, MI USA
(2) Climate and Space Dept., University of Michigan, Ann Arbor, MI USA

ABSTRACT

A new method for estimating the center of tropical cyclones is presented. The algorithm fits a parametric model of the wind field to wind speed observations by the Cyclone Global Navigation Satellite System (CYGNSS) and adjusts the assumed storm center in the model to minimize the residual difference between observations and model. The performance of the estimator is improved by using an ensemble averaging approach to account for uncertainties in the first guess storm center location provided by the National Hurricane Center (NHC). A performance analysis indicates that the NHC uncertainty is reduced by greater than a factor of 4 using the new storm center estimator.

Index Terms— CYGNSS, GNSS-R, Tropical Cyclone, Storm Center, Remote Sensing

1. INTRODUCTION

CYGNSS is a constellation of eight satellites that were successfully launched on 15 December 2016 into an orbit plane at 35° inclination. It measures surface winds by receiving GPS signals reflected from the ocean surface. It functions in tropical cyclones because the GPS L1 wavelength (19 cm) is largely unattenuated by heavy precipitation. CYGNSS measurements are suitable for determining storm center location because of their short median and mean revisit times of 3 and 7 hours, respectively. For more on CYGNSS, see [1].

NHC best-track estimates are official records of tropical cyclone intensity, position, wind radii, and more, which are created from post-storm analysis. The best-tracks have many applications, including tropical cyclone model verification, climate change studies, insurance studies, and forecasting [7]. It is important for the best-track estimates to be as accurate as possible. Best-track estimates of storm center location is of particular interest for this study.

Current methods for obtaining storm center fixes include using aircraft reconnaissance, satellite

data from microwave imagers, scatterometers, and sounders to make estimations. Cases with aircraft reconnaissance data have the lowest uncertainty in storm center, but they are only available for less than 30% of storms in the Atlantic basin, and for no storms in other basins. With current methods, determining the storm center location is difficult when the storm is not well organized, or when the eye is obscured by cirrus clouds or has a tilted eyewall so that it is not clearly visible in satellite imagery [6]. However, surface wind speed measurements can still be made with CYGNSS under these conditions, so storm center fixes derived from those data could still perform well when other methods are hindered.

2. ALGORITHM

The storm center location is estimated by fitting a parametric model of the wind field to CYGNSS wind speed observations, while adjusting the assumed storm center in the model to minimize the residual difference between observation and model. First, CYGNSS data are divided into 3-hour intervals for each storm center fix. Next, an initial guess for storm center location is assigned to the center of the 3-hour interval based on linear interpolation of 6-hourly NHC best-track estimates. The storm is assumed to move in a straight line and with constant velocity between the adjacent best-track centers. This fixes the angle of the storm's direction of movement and its position as a function of time between the two 6-hr end points. Although the storm center location is actually a function of time, for brevity in the remainder of this paper we will refer to a single storm center location at the center of the 3-hour interval. The CYGNSS data are relocated in storm-centric coordinates using the time-dependent storm center location at the time of each data sample. Next, the CYGNSS wind speed observations are fit to a parametric model following the approach described in [2]. The model assumes a radially

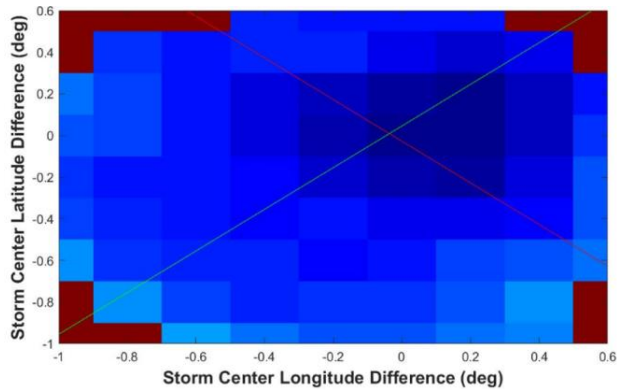


Figure 1: A typical fit of a 2-dimensional Gaussian (represented by the crossing red and green lines) to the RMSE error surface. The point (0,0) is where the first guess of storm center location is. The search area is +/- 1° around this point. Some of that area is not shown because it was masked out (red squares indicate that area contains fits with a radius of maximum winds > 100 km). Intersection of the two Gaussians is the storm center solution. Dark blue is the minimum RMSE, or best result.

dependent wind field with azimuthal symmetry, as given by

$$V(r) = \frac{2r(R_m V_m + .5fR_m^2)}{R_m^2 + ar^b} - \frac{fr}{2} \quad (1)$$

where r is the distance from storm center of each wind speed measurement, f is the Coriolis factor, R_m is the radius of maximum winds, and V_m is the maximum wind speed. The exponent b controls the rate at which the winds radially decay. The factor a can be solved from the other factors by requiring that maximum value of $V(r)$ be equal to V_m , so this is effectively a 3-parameter model, with parameters b , R_m , and V_m . The model fit uses least squares minimization over the 3-dimensional parameter space. The quality of fit is determined as the root mean squared residual difference between the model and observations.

The storm center location is estimated as a brute force search over a range of possible storm centers. For each potential storm center location, the residual of the model fit is determined. The estimated storm center has the lowest residual. The domain of the search is a +/- 1° window in latitude and longitude centered on the NHC best-track estimate.

The model fit residual as a function of the assumed storm center forms a 2-dimensional error surface. Models with a radius of maximum winds greater than 100 km are discarded from the error surface as being non-physical. They can appear with low residual values because, when fitting to data far

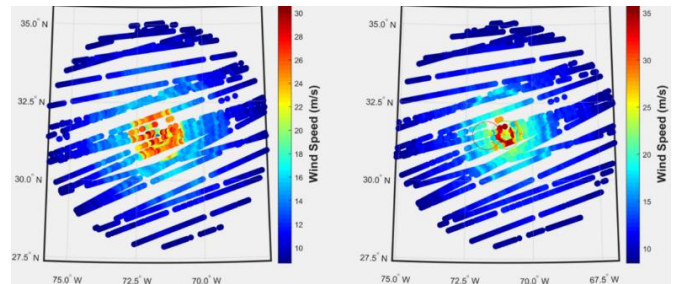


Figure 2: The wind field for Hurricane Jose on 17 Sept 2017 at 18:45 UTC (3 hours of CYGNSS data). Left image uses the original storm center from NHC interpolation while the right image uses the new storm center found by the algorithm. Both images are radially smoothed over 10 km. In the right image, the red circle represents the original center, and the green circle is the new center.

from the true storm center, the population is mostly low wind speed data with much less noise than the high wind speed data. This allows for a fit with very low RMSE, but it cannot be the storm center because it is unphysical for a tropical cyclone. Tropical cyclones almost always have a radius of maximum winds well below 100 km, and typically around 50 km [5]. After applying this mask, a 2-dimensional Gaussian function is fit to the residual error surface as in Figure 1. Note that a 2-dimensional Gaussian is appropriate because there is typically a well-defined local minimum with a steady roll-off away from the minimum, as seen in Figure 1. The point where the best-fit Gaussian is minimum is the estimated storm center location for the middle of the 3-hour data interval.

The process described above is a complex, nonlinear algorithm where perturbations in initial conditions can result in unpredictable, small changes in residual and storm center location. To improve the storm center fix and to calculate the uncertainty of the solution, an ensemble approach is used much like in weather forecasting [3,4]. In this Monte Carlo ensemble approach, the NHC storm centers are perturbed in position, and the storm location estimator is re-run. The ensemble average storm center location is taken as the mean location over all Monte Carlo trials.

3. RESULTS

Figure 2 demonstrates the impact of moving the storm center from the original location, determined by simple linear interpolation between two 6-hr NHC best-track locations, to the new estimated location. Both images show the wind field of all CYGNSS measurements in a

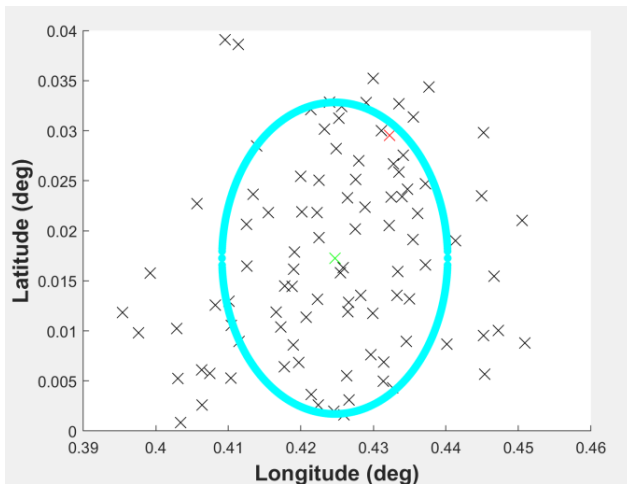


Figure 3: A typical result of Monte Carlo trials. The point (0,0) is the first guess at the storm center location. Each 'x' represents where the new storm center was found to be. The red 'x' is where the storm center was found on the first trial, without perturbing the NHC storm centers. The green 'x' is the mean of all other trials. The cyan circle has a radius of the standard deviation of all trials relative to the green 'x'. This case had a NHC storm center uncertainty of 10 km and uses the same CYGNSS data as Figure 2.

3-hour window. The left image has the original storm center while the right image has the new storm center determined by the algorithm. Both images have been radially smoothed over 10 km. The winds near the center of the original wind field have approximately uniform wind speeds over more than a 150 km diameter. This is not characteristic of a typical tropical cyclone. After adjusting the storm center, the strongest winds appear in a circle of much smaller diameter, the winds radially decay as expected, and the calm winds in the eye become visible. Note that it is reasonable to expect CYGNSS to be able to resolve eyes of TCs because the footprint of the satellite is typically about 25 km whereas eyes can be 60 km or larger in diameter. [1]

Monte Carlo trials were run with each trial perturbing the two storm center locations from NHC. The storm centers are randomly perturbed using an additive, zero-mean Gaussian distribution for distance and a uniform $[0, 360^\circ]$ distribution for heading. The standard deviation of the Gaussian distribution is a parameter that is varied to assess the sensitivity of the final estimate to uncertainty in the initial NHC locations. Note that the two NHC storm centers are varied independently. 1000 trials were run for Gaussian standard deviations of 10, 25, 40, 55, and 70 km. These uncertainties cover the range typically seen in the best-track forecast [7].

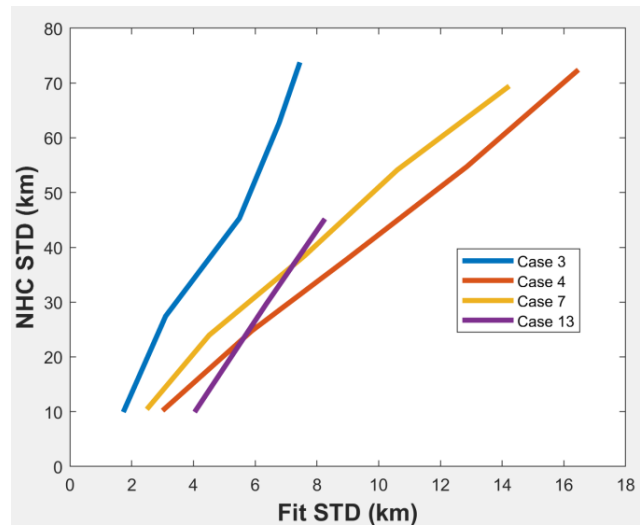


Figure 4: The effect of NHC storm center uncertainty on the standard deviation of the resulting storm center found by the algorithm in this paper for 4 different cases which represent different storms, times, and CYGNSS samples. The slope of each line represents the improvement in uncertainty of storm center. The slopes of these lines are 11.0, 4.6, 5.0, and 8.4 for cases 3, 4, 7, and 13, respectively.

The trials demonstrated great robustness and consistency as seen in Figure 3, which is a typical result. The 'x's mark the storm center that was found in each trial. The point (0,0), which is not shown on the plot, is the initial guess at the storm center location from linear interpolation of NHC storm centers. The red 'x' is the storm center that was found in the first trial, without the ensemble approach or perturbations of NHC storm centers. The green 'x' is the mean of all trials which is taken to be our best estimate of storm center location. This green 'x' is approximately 47 km from the origin. Note that this does not necessarily imply that NHC's storm center locations were off by 47 km. There could also be errors associated with the assumption of uniform storm center motion with constant velocity during the 6-hr time interval between best-track fixes. The uncertainty of the storm center in this case, given by the standard deviation of all trials in Figure 3, is 1.73 km, which is a factor of 5.8 improvement over the NHC uncertainty of 10 km. Also note that the ensemble approach moved the storm center solution by ~ 1.7 km and reduced the uncertainty of the result from 2.36 km to 1.73 km.

The plot in Figure 4 shows how the standard deviation of the storm center resulting from the Monte Carlo trials changes as a function of the standard deviation of NHC storm center location. This is shown for 4 different cases. The slope of these lines represents

the improvement factor in the confidence in the storm center for this algorithm over NHC. Depending on the sampling and depth of the minimum in the residual error surface, this algorithm improves upon the NHC storm center by a factor of between 4 and 11.

4. CONCLUSION

A new method for finding the storm center of tropical cyclones is presented, and results indicate a factor of between 4 and 11 improvement in uncertainty compared to current NHC storm center fixes.

Future work includes optimizing the 100 km radius of maximum winds threshold as well as the 2-degree latitude/longitude search space. Another improvement could be to make the algorithm independent of NHC's storm center estimates (this is necessary for near real time storm center fixes). Storm center accuracy might improve if the trajectory of the storm were not limited to a straight line. It would also be very useful to know how the uncertainty in storm center location changes with respect to things like storm strength, storm organization, and number and distribution of wind speed measurements.

6. REFERENCES

- [1] C.S. Ruf, et al., "New Ocean Winds Satellite Mission to Probe Hurricanes and Tropical Convection," *Bull. Amer. Meteor. Soc.*, doi:10.1175/BAMS-D-14-00218.1, pp. 385-395, Mar 2016.
- [2] M. Morris, C.S. Ruf, "Determining Tropical Cyclone Surface Wind Speed Structure and Intensity with the CYGNSS Satellite Constellation," *Journal of Applied Meteorology and Climatology*, DOI: 10.1175/JAMC-D-16-0375.1, pp. 1847-1865, Jul 2017.
- [3] Z. Zhang, T.N. Krishnamurti, "Ensemble Forecasting of Hurricane Tracks," *Bull. Amer. Meteor. Soc.*, pp. 2785-2796, Vol 78, No 12, Dec 1997.
- [4] Z. Zhang, T.N. Krishnamurti, "A Perturbation Method for Hurricane Ensemble Predictions," *Monthly Weather Review*, Washington Vol 127, Issue 4, pp. 447, Apr 1999.
- [5] F. Lajoie, K. Walsh, "A Technique to Determine the Radius of Maximum Winds of a Tropical Cyclone," *Weather and Forecasting*, DOI: 10.1175/2008WAF2007077.1, Volume 23, pp. 1007-1015, Oct 2008.
- [6] R. Torn, C. Snyder, "Uncertainty of Tropical Cyclone Best-Track Information," *Weather and Forecasting*, DOI: 10.1175/WAF-D-11-00085.1, Boston Vol. 27, Iss. 3, pp. 715-729, Jun 2012.
- [7] C.W. Landsea, J.L. Franklin, "Atlantic Hurricane Database Uncertainty and Presentation of a New Database Format," *Monthly Weather Review*, DOI: 10.1175/MWR-D-12-00254.1, Vol. 141, pp. 3576-3592, Oct 2013.